TUDelft

Delft University of Technology

Advanced high strength steels
Improved properties by design of textures and microstructures

Kestens, Leo; De Knijf, Dorien; Castro Cerda, Felipe; Petrov, Roumen

Important note
To cite this publication, please use the final published version (if applicable).
Please check the document version above.

PAPER • OPEN ACCESS

Advanced High Strength Steels: Improved Properties by Design of Textures and Microstructures

To cite this article: Leo A.I. Kestens *et al* 2017 *IOP Conf. Ser.: Mater. Sci. Eng.* **219** 012004

View the article online for updates and enhancements.

Related content

- Influence of heating rate and temperature on austenite grain size during reheating steel
  Richard A.M. Napitupulu

- 3D phase field modelling of recrystallization in a low-carbon steel
  B Zhu and M Militzer

- Realizing Ultrafine Grained Steel by Simple Hot Deformation Using Dynamic Transformation and Subsequent Dynamic Recrystallization Mechanisms
  L Zhao, N Park, Y Tian et al.

Recent citations

- Effects of untransformed ferrite on Charpy impact toughness in 1.8-GPa-grade hot-press-forming steel sheets
  Min Cheol Jo *et al*

Advanced High Strength Steels: Improved Properties by Design of Textures and Microstructures

Leo A.I. Kestens[1,2], Dorien De Knijf[1,3], Felipe Castro Cerda[1,4] and Roumen H. Petrov[1,2]

[1]Ghent University, EEMMeCS Dept, Technologiepark 903, 9052 Gent, Belgium
[2]Delft University of Technology, Materials Science and Engineering Dept, Mekelweg 2, 2628 CD Delft, The Netherlands
[3]ArcelorMittal – Gent, John F. Kennedylaan 51, 9042 Gent, Belgium
[4]Universidad de Santiago de Chile, Department of Metallurgical Engineering, Av. Lib. Bdo. O´Higgins 3363, Estación Central, Santiago de Chile, Chile

leo.kestens@ugent.be

Abstract. Texture and microstructure formation during annealing of a 75% cold rolled AHS steel, reheated at a rate of 10°C/s to ~3000°C/s were studied with the purpose to investigate the interaction between the recrystallization and the austenite formation as well as the possibility of grain refinement. It was found that at ultra-high heating rates, the bcc-fcc phase transformation starts before the completion of recrystallization and the deformation texture is partially retained in the samples after annealing. The crystallographic texture observed in the martensitic phase, which is the product of intercritical austenite transformation in as-quenched samples, i.e., after the double α-γ-α' transformation, is similar to the initial cold rolling texture, which is an indication for the texture memory effect. After ultra-fast reheating with average reheating rates of 1000°C/s and higher, a significant grain refinement was observed with an average calculated ferrite grain diameter of ~2 μm. The obtained final ferrite grain size depends significantly on both the reheating temperature and the heating rate. The same effect is observed in 75% cold rolled quenching and partitioning steels for heating rates of 400°C/s, 800°C/s and 1000°C/s. In both cases the combination of fine grains, and weak RD/ND-fiber textures produce an increase of strength and ductility compared to material annealed using a conventional heating rate of ~10°C/s.

1. Introduction

The development of advanced high strength steels (AHSSs) was a reaction of the steel industry to societal requests to decrease the CO_2 emissions of the cars without sacrificing passenger safety [1]. The combination of strength and toughness is a consequence of the unique design of the microstructure in AHSS, which combines hard, ductile and metastable phases. The development of AHSS grades is one of the enduring priorities of the steel manufacturing industry today and requires often non-conventional approaches in development of stronger and tougher steel grades. The use of high strength steels in the automotive industry appears to be an effective way to decrease the weight of vehicles, to increase the safety of the passengers and to decrease the fuel consumption.
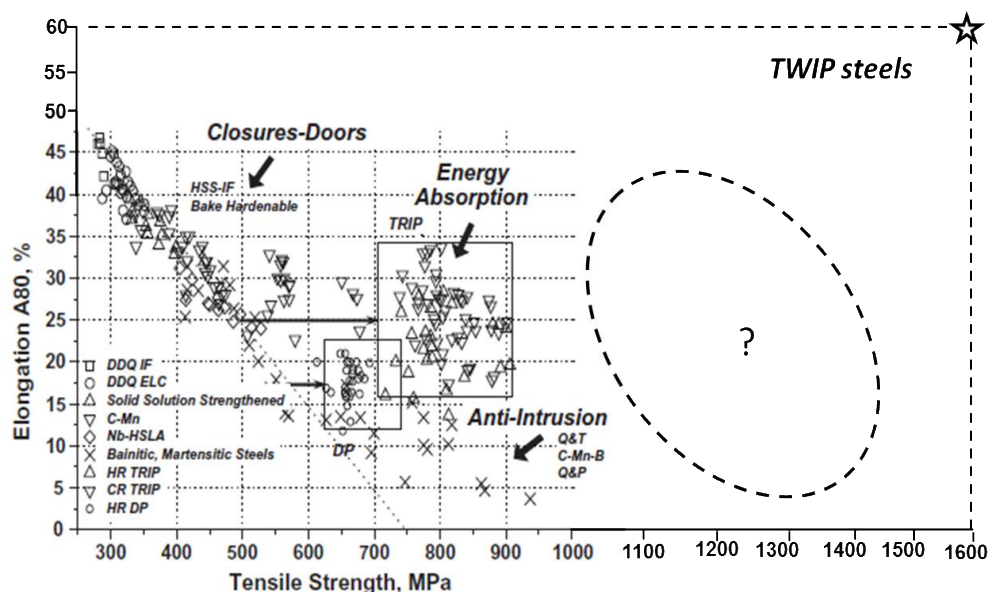
Figure 1. Distribution of the existing steel grades according their ultimate tensile strength (UTS) and tensile elongation (TE). The zone marked with a dashed ellipse is still without commercial representatives. (Adapted from ref. [2] with the data for TWIP steels).

Such steels are known as 3rd generation AHSSs and they are still under development by steel producers. The classical approach for the development of AHSS grades is two-fold, namely *(i)* the use of a specific combinations of alloying elements and *(ii)* control of the thermo-mechanical manufacturing process, which determines the formation of the microstructure. This approach appears to be very successful and has given rise to well-known steel grades such as dual phase (DP) steels, transformation induced plasticity (TRIP) steels, multiphase or complex phase steels (steels with dislocation rich microstructures such as martensite and bainite) [2] and, more recently, twin induced plasticity (TWIP) steels. The well-known strength vs ductility chart for the most popular automotive steel grades is shown schematically in Figure 1.

It is clear that there are no representatives at the moment which can cover the gap between the heavy alloyed TWIP steels and low alloyed TRIP steels. Adding of alloying elements, as done in medium Mn steels, is an easy solution, but problems with metal scarcity will restrict their extensive use more and more in the future because of cost limitations. The control of cooling rates during production is already very well studied; *i.e.*, the limits to improvement in modifying this parameter are known and significant new improvements in this direction cannot be expected, although new heat treatments like quenching and partitioning (Q&P) are now under development in order to populate the region marked with a question mark in Figure 1 [1].

A non-conventional approach is to explore the potential of the heat treatment as a tool for microstructure-properties control by using well known standard compositions and to design and produce fine grained steel grades by employing very high heating rates. This approach leads to extreme grain refinement [3–6] and to a corresponding increase of the strength of the material above the *normal* well known limits. In previous works [3–7] a number of microstructural phenomena, like remarkable grain refining and overlapping of the recrystallization with the α-γ phase transformation, were reported for reheating rates of 3000°C/s and higher (up to 7000°C/s). Although the results were very promising, it is very difficult to reproduce such heating rates in industrial lines.

The aim of the present work is to obtain a better understanding of the sensitivity of the phase transformation and recrystallization, and the corresponding changes in microstructure, texture and mechanical properties to the variation of the heating rates and initial microstructure. To study the

possibilities for an industrial implementation all processing parameters are varied in a range which is considered as realistic for industrial application.

2. Experimental

Cold rolled steel with a composition shown in Table 1 is the object of study in this work. Two sets of dual phase (DP) steel, produced as hot rolled plates with a microstructure of either (i) ferrite and pearlite (FP) or (ii) 50% ferrite and 50% tempered martensite (FM) were subsequently cold rolled with a reduction of 75%, to a final thickness of 1 mm, and heat treated according the temperatures and times shown in tables 2 and 3. Samples of size 80 x 30 x 1 mm^3 were cut parallel to the rolling direction of the cold rolled sheet. The samples were reheated with heating rates of 10°C/s, ~400°C/s and ~1500°C/s and subsequently water quenched without isothermal holding (a minimum isothermal holding of 0.2s could not be avoided). The data for the heat treatment parameters are given in Table 2 and Table 3, whereby the samples with initial microstructure of ferrite and tempered martensite are designated as samples A and the samples with initial microstructure of ferrite and pearlite are designates as samples B. A record of the real "time-temperature" curves is shown as an example in Figure 2.

Q&P samples (100 x 10 x 0.5 mm^3) were 80% cold rolled and subsequently subjected to ultra-fast heating (UFH) Q&P cycles in the Gleeble™ thermo-mechanical simulator according to the cycles shown in Figure 3. Two types of heat treatments were applied: one with isothermal soaking and the other without isothermal soaking, (cf. Figure 3).

**Table 1**. Chemical composition of studied steels, in mass. %.

	%C	%Si	%Mn	%P	%S
DP (FM and FP)	0.114	1.263	2.072	0.0149	<0.001
Q&P	0.25	1.5	3.02	0.015	<0.001

**Table 2**. Heat treatment parameters and hardness of samples with microstructure 75% cold rolled F+TM.

Sample ID	Heating temperature Ta, °C	Heating rate, Vh °C/s	Quench rate, V_q, °C/s	HV3
A0	-	-	-	440
A1	674	430.2	-1281.7	405
A2	723	397.8	-821.9	360
A3	756	397.5	-1069.3	359
A4	780	328.7	-568.2	341
A6	807	357.5	-735.8	354
A7	846	323.4	-836.0	402
A8	879	317.3	-854.2	510
A9	949	352.9	-1064.4	561
A10	968	359.9	-1068.9	512
AVERAGE		362.8	-922.3	

Table 3. Heat treatment parameters and hardness of samples with microstructure 75% cold rolled F+P.

Sample ID	Heating temperature Ta, °C	Heating rate, V_h °C/s	Quench rate, V_q, °C/s	HV3
B0	-	-	-	329
B1	749	1567.6	-803.2	329
B2	841	1445.5	-1390.2	442
B3	862	1327.5	-1539.7	421
B4	1000	1419.0	-966.9	549
B5	1053	1538.1	-1058.7	545
B6	1200	1532.2	-685.4	507
AVERAGE		1471.7	-1074.0	
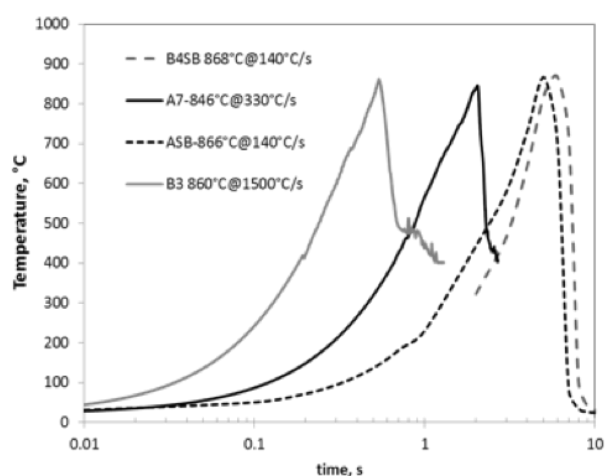
Figure 2. Record of time-temperature curves for samples with initial microstructures ferrite and tempered martensite (A) and ferrite and pearlite (B), heated in the salt-bath furnace (140°C/s) and at ulta-fast heating rates of 330°C/s and 1,500°C/s.
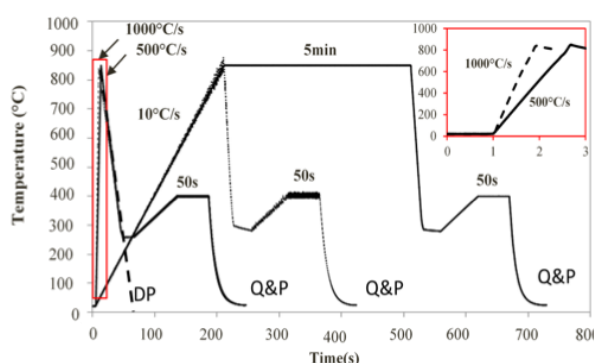
Figure 3. Heat treatment cycles performed in Gleeble on the cold rolled material, upper right corner insert is a zoom of the first 3s of heating time. The cooling rates for DP steel and for Q&P steel are marked with DP and Q&P correspondingly. Adapted from [8].

Samples for tensile tests, hardness tests and microstructure characterization were taken from the middle part of the heat-treated sheets from the zones with guaranteed homogeneous temperature distribution. Sub-size tensile test samples with a gauge length of 4 mm, width of 1mm, thickness of 1mm and total length of 10 mm were tested with a cross head velocity of 0.5 mm/min at room temperature in a micro-tensile test machine (type *Deben MICROTEST 5000N Tensile stage®*). The sample elongation was detected by displacement measurement of the machine grips. Tensile tests on sub-size samples always overestimates the strength and elongation in comparison to the standard size (A80 and A50) tensile test samples.

Similar tensile tests were applied to specimens that were water quenched from different temperatures after reheating with fast but still conventional heating rates of 140°C/s in a salt bath (SB), in order to compare the results with the data obtained from ultra-fast heating, and to correctly evaluate the contribution of ultra-fast heating to the mechanical properties. The microstructural characterization was carried out after classical metallographic sample preparation, which included mechanical grinding and polishing up to 1 μm diamond suspension and etching with 2% HNO_3 in ethanol (Nital 2%).

Samples for electron backscatter diffraction (EBSD) characterization were additionally electrolytically polished using a Struers® Lectropol 5 device with A2 type electrolyte at 22°C, 40V and electrolyte flow rate of 7. A FEI-Nova 600 scanning electron microscope was employed for the scanning electron microscope (SEM) and EBSD data acquisition on selected samples. The EBSD data were acquired at 15 kV, working distance 7 mm, sample tilt 70°, on a square scan grid with a step size of 50 nm. The data were post-processed with EDAX-TSL OIM® 5.1 data analysis software. The variations in mechanical properties as a function of quench temperature were documented by Vickers hardness measurements with a load of 3 kgf (HV3).

3. Results and Discussion

3.1. DP steel samples: microstructures
Variations in the hardness of the cold rolled and water quenched samples with different initial microstructures after heating to different temperatures with various heating rates are shown in Figure 4. The initial hardness after cold rolling depends on the microstructure and is 329HV3 for the samples

from group B with ferrite-pearlite microstructure, compared to 440HV3 for the cold rolled microstructure of ferrite and tempered martensite. The hardness does not change significantly after quenching from a temperature up to 500°C (Figure 4, zone I). An increase of the temperature with heating rates of 140°C/s (heating in a salt bath) triggers initially recovery and recrystallization in the cold rolled steel, which is associated with a decrease in the hardness (cf. Figure 4, Zone II). After quenching from temperatures situated in the dual phase ferrite-austenite or the single phase austenite regions, the hardness increases due to martensite formation from the parent austenite phase (cf. Figure 4, zone III). When the austenitisation temperature is very high the hardness after quenching slightly decreases, which can be associated with the grain growth of the parent austenite, which forms coarse and low carbon martensite (Figure 4, zone IV).

Two main tendencies are clearly demonstrated in the hardness variations – apart from the heating temperature the hardness variations are dependent on: *(i)* the initial microstructure, and *(ii)* on the heating rate. The increase of the heating rate from 140°C/s to ~360°C/s and 1500°C/s shows a clear tendency to increase the hardness after quenching from both the intercritical (α+γ) and the single phase γ regions. The hardness decrease in the temperature interval 500-750°C (zone II in Figure 4), which is associated with recovery and recrystallization, becomes smaller when the heating rate is increased, which indicates that recovery and recrystallization are suppressed. No changes in the hardness are observed in samples B that were heated to the austenitic region with ~1500°C/s (cf. zone II in Figure 4- the grey line for heating rate of 1500°C/s). This is an indication that both recovery and recrystallization are completely suppressed and the α-to-γ phase transformation starts before the onset of recrystallization. This effect was previously observed after heating and quenching of cold rolled high-strength low-alloy (HSLA) steels with heating rates of ~3000°C/s and ~7000°C/s [4–7].
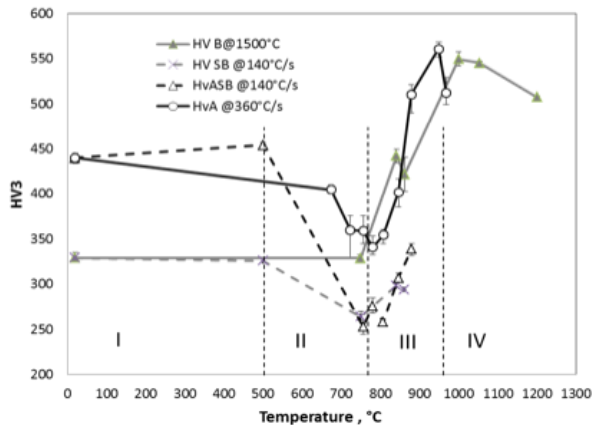
The tensile test results for selected samples are shown in Figure 5. The samples were water quenched from the temperatures of the two-phase (α+γ) region in order to create a microstructure of ferrite and martensite, which is typical for DP steels [1,2]. It is clearly demonstrated that for intercritical annealing, an increase of the heating rate from 140°C/s to 400°C/s and 1500°C/s causes a significant increase in the ultimate tensile strength (Rm). This phenomenon could be associated with the significant grain refining effect observed in the fast-heated samples in comparison to the samples heated in the salt bath. A second important observation is that the short soaking times, practically ~1-2 s in both cases, do not allow homogenization of the carbon content of the intercritical austenite before quenching. This means that the martensite "islands" are structurally heterogeneous — i.e. they may contain zones with high carbon martensite, low carbon martensite or even retained austenite with high carbon content and correspondingly with different hardness [9].

Another relevant observation is that the initial microstructure has significant effect on the mechanical properties (type of the tensile test curve), which is more clearly pronounced at low heating rates. The tensile test curves of samples with initial ferrite and pearlite microstructures, quenched after heating with 140°C/s exhibit a well-defined yield point, and display very low work hardening, which is different in the samples with initial microstructure of ferrite and tempered martensite. It is also important to mention that the stress-strain curves reveal identical characteristics after ultra-fast heating (compare the black thick and dashed lines in Figure 5).

Figure 6 shows the microstructural evolution in samples with initial microstructure of ferrite and tempered martensite after water quenching from various temperatures in α+γ temperature interval reached with heating rates of ~140°C/s (heating in a salt bath) and fast heating with ~400°C/s. The micrographs display martensite microstructures in both group of samples, which in the case of fast heating (Figure 6b,c) appear in the recovered ferrite matrix, and the new martensite is aligned along the pancaked recovered (or partially recrystallized) ferrite. In the case of heating in the salt bath, the ferrite microstructure is fully recrystallized with well-developed almost equiaxed grains shape (cf. Figure 6d, e). The microstructures shown in Figure 7(a-e) display the corresponding changes in the steel with 75% cold rolled ferrite-pearlite microstructure after heating with ~1500°C/s and 140°C/s. The same tendency is clearly demonstrated, namely the α-to-γ phase transformation during heating starts before the onset of the recrystallization in samples heated with 1500°C/s, resulting in a fine-

grained microstructure with elongated partially recovered ferrite grains, whereas after reheating in a salt bath the phase transformation develops in the recrystallized ferrite–pearlite matrix.

Figure 4. Hardness vs. quench temperature for different initial microstructures and heating rates. "Quench temperature" is the temperature to which cold rolled samples were heated before water quenching.
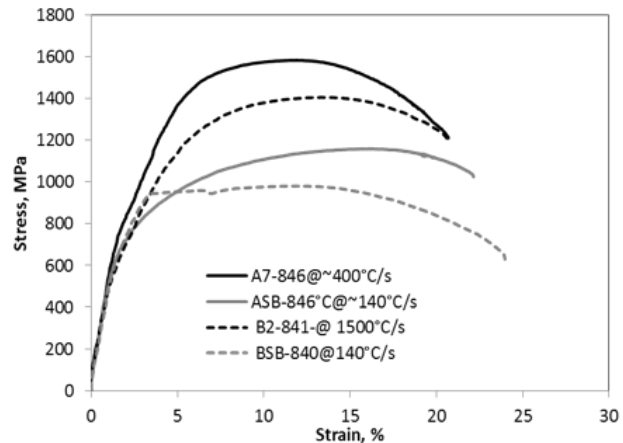
Figure 5. Tensile test results from water quenched samples after ultra-fast heating with rates of ~400°C/s and 1500°C/s (A7 and B2) and after conventional fast heating in a salt bath with ~140°C/s (samples ASB and BSB). All samples are heated for quenching to similar temperatures (~840°C) in the dual phase α+γ temperature region.
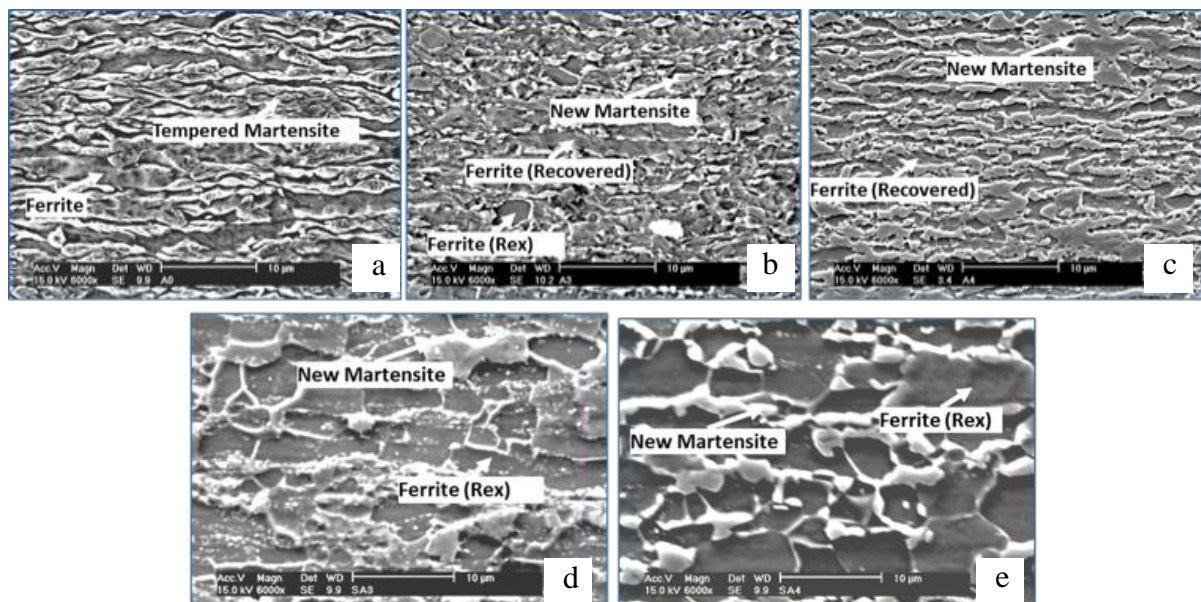
Figure 6. Microstructures of samples A and ASB (initial microstructure ferrite and tempered martensite) after: 75% cold rolling (a); reheating with ~400°C/s to 756°C (b); to 780°C (c); reheating with 140°C/s in salt bath to 756°C (d) and780°C(e). All samples are subsequently water quenched without isothermal soaking. Scale bar in all micrographs is 10μm.
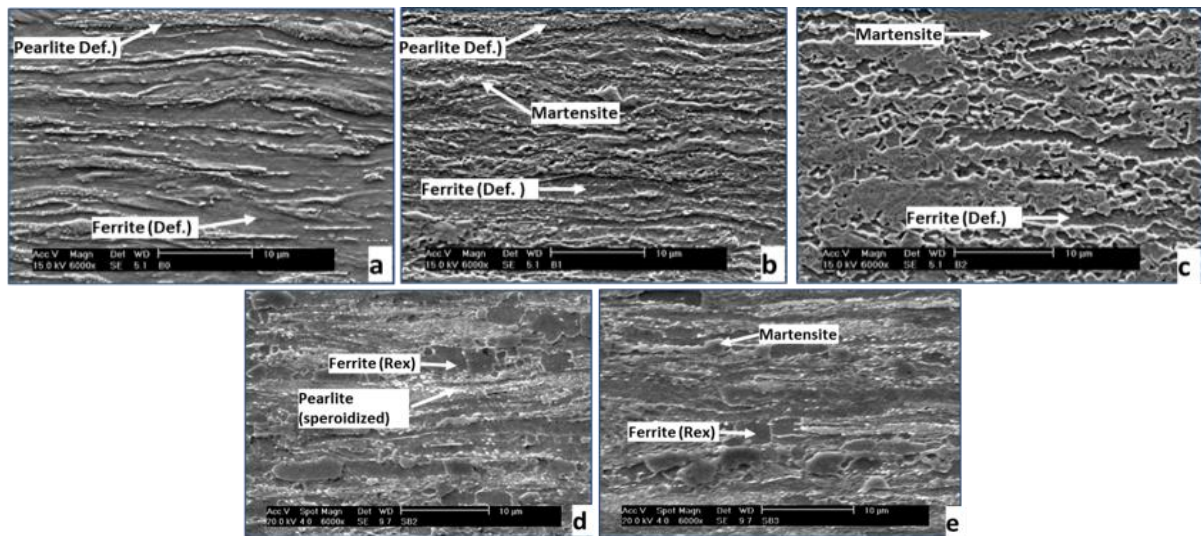
Figure 7. Microstructures of samples B and BSB (initial microstructure ferrite and pearlite) after: 75% cold rolling (a); reheating with ~1500°C/s to 750°C (b); to 840°C (c); reheating with 140°C/s in salt bath to 756°C (d) and 840°C (e). All samples are subsequently water quenched without isothermal soaking. Scale bar in all micrographs is 10 µm.

The evolution of the average ferrite grain size as a function of the heating rate was investigated on optical and SEM micrographs by means of the linear intercept method and a cross check of the result was made by EBSD measurement on samples A3 (cf. Figure 8-black triangle). The results of the measurement, which are shown in Figure 8, display that the average grain size drops from 5 µm to 1 µm with an increase of the heating rate from 140°C/s to 1500°C/s reaching a steady state. The last point in the figure represents data adopted from reference [6] for steel with the same chemical composition heated to the same temperatures with 3000°C/s.

3.2. DP steel samples: textures
Figure 9a shows the key for the main BCC texture components in the $\phi2 = 45°$ section of Euler space and Figure 9b displays the orientation distribution function (ODF) of the 70% cold rolled initial material. Figure 9b shows a typical rolling texture with ND {111}<uvw> and RD {hkl}<110> fibers with an intensity of ~4.5 multiples of random density (mrd) [10].

Figure 10 illustrates only the ferrite textures derived from the EBSD scans using grain average image quality partitioning criteria [22]. Figure 10a, 10c, 10e, and 10g show the ODFs of the full ferrite phase (including both recrystallized and non-recrystallized grains), whereas Figure 10b, 10d, 10f, and 10h show the ODFs of recrystallized ferrite grains only. The recrystallized ferritic grains were extracted using the grain average misorientation (GAM) criterion [18, 23]. The recrystallized ferrite grains in samples heated at 150°C/s (cf. Figure 10b, 10d) show orientations close to {111}<uvw> ND fiber components. In samples heated at 150°C/s to 704 °C, the recrystallized grains have an orientation in the vicinity of the {111}<112> texture components (Figure 10b), whereas the strongest intensity after heating to 838°C at 150°C/s is 7.1 mrd and belongs mainly to the {001}<110> components.

The ODF of ferrite in samples heated at 1500°C/s to 749°C (Figure 10e) is very similar to the ODF of the cold-rolled initial material (Figure 9b). Figure 10f shows the ODF of ferrite at a very early stage of recrystallization in a sample heated at 1500°C/s. The maximum intensities of 3.1 mrd are close to {112}<110> texture component. The ODF of samples heated at 1500°C/s to 862°C (cf. Figure 10g) shows that the ferrite texture intensities are similar to the cold-rolled texture in the main components of ND {111}<uvw> and RD {hkl}<110> fibers. Recrystallized grains in the same sample show strong intensities on the {112}<110> and {111}<112> components (cf. Figure 10h).
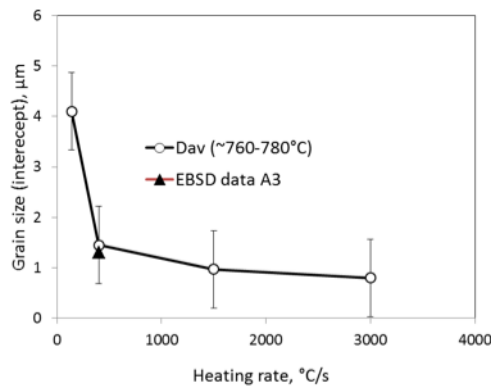
Figure 8. Average grain size (average intercept length) after water quenching as a function of heating rate. Black triangle shows average grain diameter measured from EBSD data.
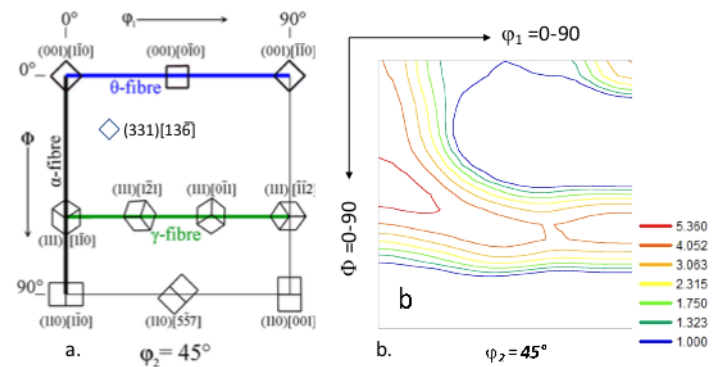
Figure 9. (a) Ideal positions of the most important BCC texture components in the $\phi2 = 45°$ section of Euler space and (b) plot of ODF of the cold rolled steel used in this work.

The appearance of the Goss {110}<001> texture component with intensity of ~1.7 mrd is observed after heat treatments at both heating rates (cf. Figure 10b, 10d, and 10h). The Goss component is associated with oriented nucleation at shear bands in deformed ferrite [11]. The rotated Goss {110}<110> component, which is a high stored energy component for metals with BCC crystal structure after plane-strain compression, appears in the recrystallized ferrite after UHF at 1500°C/s (cf. Figure 10f and Figure **10**h). These components are claimed to originate along shear bands in deformed ferrite [11–13]. In some recrystallized ferrite textures also the {331}<136> component can be observed (cf. Figure 10b, Figure **10**d, Figure **10**f, and Figure **10**h). This component has been described already before [14] and is supposed to originate from specific deformation features, like intra-grain deformation bands in deformed ferrite {hkl}<110> fiber grains.

Texture measurements have shown that the first recrystallized grains of ferrite in samples treated at 150°C/s to 704°C are mainly oriented around the {111}<112> component (cf. Figure 10b). It is well known that such orientations are the most frequently occurring recrystallization component in cold-rolled low carbon steel [12,15]. Grains oriented close to {001}<110> are also present, which might be due to nucleation at low stored energy grains [16] at the beginning of recrystallization. Grains with Goss {110}<001> texture component have nucleated and grown in samples heated at 150°C/s (cf. Figure 10b).
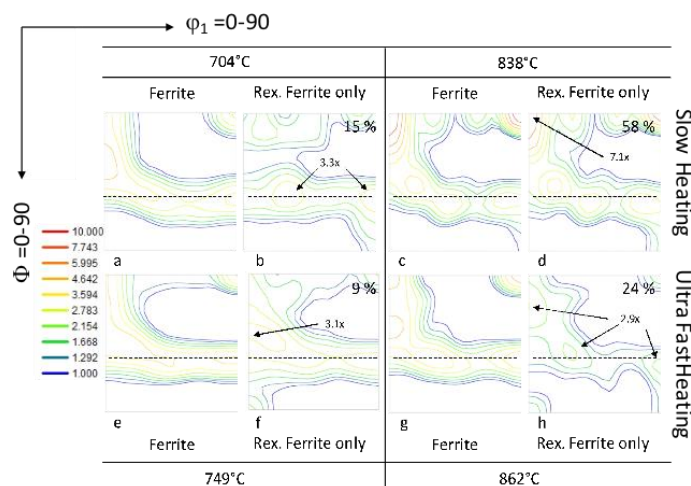
Figure 10. ODF of ferrite at $\phi2 = 45°$ from samples heated at 150°C/s (a–d) and 1500°C/s (e–h). (a) and (b) correspond to peak temperature of 704°C; (c,d) to 838°C; (e) and (f) to 749°C and (g) and (h) to 862°C. (a,c,e,g) correspond to recrystallized and non-recrystallized ferrite, whereas (b,d,f,h) correspond to recrystallized ferrite. Numbers in (b,d,f,h) indicate the recrystallized ferrite fraction. Dashed line indicates the ideal position of {111}<uvw> ND fiber.

Figure 11 and Figure **12** display EBSD maps of the samples heated at 150°C/s and 1500°C/s, respectively, to different temperatures. RD-Inverse Pole Figure (IPF) maps are plotted on top of IQ maps in Figure 11a, 11c and Figure **12**a, Figure **12**c. In these maps only the grains oriented close to the Goss {110}<001> (Figure 11a, 11c and Figure **12**c) and rotated Goss {110}<110> (Figure 12a) components with a tolerance of 10° from the ideal orientations are highlighted on the IQ maps. Figure 11b, Figure **11**d and 12b, 12d show the corresponding ND-IPF maps for each IQ map on the left-hand side. With help from the color coded RD-IPF maps, grains oriented close to the Goss texture component can be identified in the microstructure as the reddish grains in Figure 11a, Figure **11**c and 12c and greenish in Figure 11b, Figure **11**d and 12d. Grains oriented close to the rotated Goss component can be identified in the microstructure as greenish grains in Figure 12a and 12c and light blue grains in Figure 12b and 12d. Arrows indicate grains with Goss orientation and dashed circles the grains with Rotated Goss orientation in Figure 11 and Figure **12**.

Figure 11a and 11b show the recrystallized ferritic grains oriented close to the Goss {110}<001> component in the sample heated at 150°C/s to 704°C. The grains are aligned with other recrystallized grains at an angle of ~45° with RD (arrows). One could thus infer that grains oriented close to the Goss {110}<001> component in samples heated at 150°C/s are likely to originate from shear bands. Recrystallized ferritic grains oriented close to the Goss {110}<001> component are not observed in samples heated at 1500°C/s to 749°C. However, Figure 12c and 12d display grains oriented close to the Goss {110}<001> orientation with similar alignments as in Figure 11a and 11b. It can, therefore, be suggested that nucleation of ferrite at shear bands is delayed to higher temperatures in samples heated to 1500°C/s, compared to samples heated at 150°C/s.

The diffusion of carbon might also play a role in the nucleation of grains oriented in the vicinity of the Goss {110}<001> component in samples heated at 150°C/s (cf. Figure 10b) and at higher temperatures in samples heated at 1500°C/s (cf. Figure 10h). It has been claimed [17] that carbon dissolved in the cold-rolled ferrite strengthens the Goss {110}<001> component in recrystallized ferrite. The longer annealing times involved in samples heated at 150°C/s, compared to samples heated at 1500°C/s, can produce significant diffusion of carbon in ferrite and thus enhance the early appearance of Goss orientation in samples heated at 150°C/s. Consequently, the fact that grains with Goss orientation nucleate at higher temperatures in samples heated at 1500°C/s, is possibly affected by the carbon diffusion into ferrite.

In the sample heated at 1500°C/s to 749°C (cf. Figure 10f), the highest intensity in the ODF is located in the vicinity of the {112}<110> component. However, considerable intensities are present for Φ-values in the range from 0° to 90° for $\varphi_1 = 0$, and for the {111}<uvw> ND fiber components. It is suggested that the nucleation of the previously mentioned components is related to the stored energy in cold rolled ferrite. Under ultra-fast heating, the time for recovery in the cold rolled material is drastically reduced. The release of energy during the recovery is also reduced, and thus high stored energy components can nucleate preferentially. In cold rolled ferrite, the amount of energy that a component can store increases as Φ increases from 0° to 90° for $\varphi_1 = 0$ [17]. The maximum strain energy is accommodated by the rotated Goss {110}<110> component, which is present in the recrystallization textures of samples heated at 1500°C/s (cf. Figure 10f). The recrystallized ferrite from the sample heated at 150°C/s to 704°C (cf. Figure 10b) does not exhibit high stored energy components ($\Phi \rightarrow 90°$ for $\varphi_1 = 0$). This is believed to be a consequence of the larger time for recovery, compared to samples heated at 1500°C/s. The observed texture changes at 1500°C/s are consistent with data on ultra low carbon (ULC) steel under ultra-fast heating rates [18].
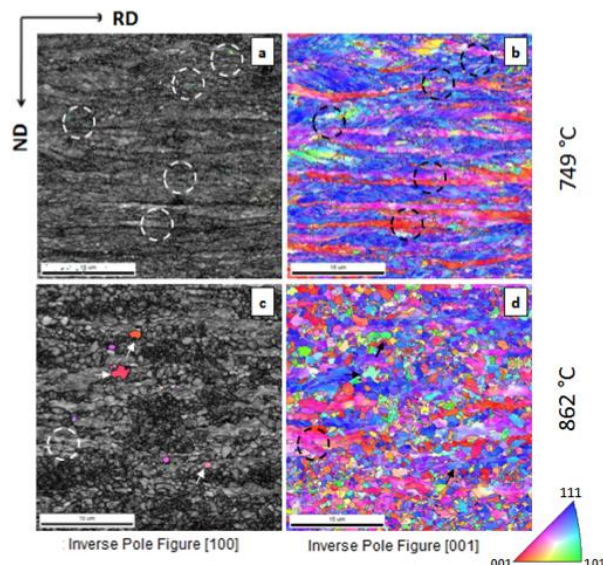
Figure 10h shows that grains oriented close to the rotated Goss component are still present in samples heated at 1500°C/s to 704°C and 862°C. The circles in Figure 12a and Figure **12**c indicate that such grains nucleated at grain boundaries. Moderated intensities are also observed in the sample heated at 1500°C/s to 862°C (cf. Figure 10f) in components close to {001}<110> and {113}<110>. These components were very weak at 749°C, which indicates that nucleation in some low stored energy {hkl}<001> RD fiber components is taking place at high temperatures. The appearance of similar low stored energy {hkl}<001> RD fiber components of recrystallized ferrite are observed in

samples heated at 150°C/s to 838°C (cf. Figure 10d). These observations are consistent with the structures, shown in figure 7, which show that nucleation accounts for a considerable fraction of the recrystallized ferrite in samples heated at 150°C/s and 1500°C/s.
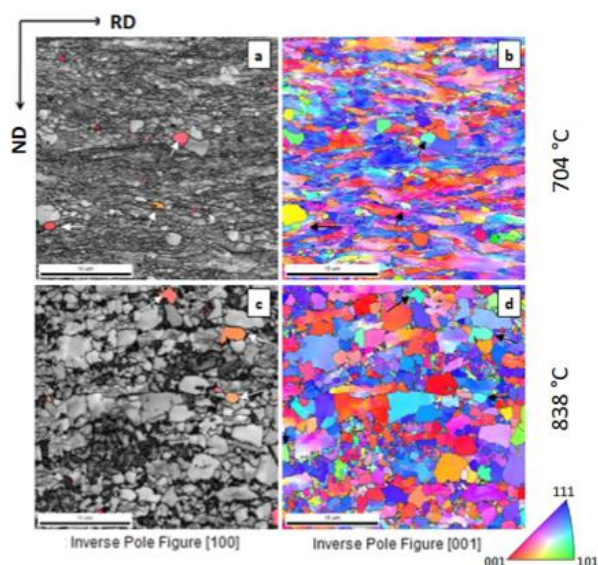
Figure 11. Microstructure of samples heated at 150°C/s to 704°C (a,b); and to 838°C (c,d). The microstructure consists of a mixture of ferrite and martensite. Arrows indicate grains oriented close to the Goss {110}<001> (with a tolerance of 10°). (c,d). (a,c) correspond to IQ maps in which the recrystallized grains of ferrite are highlighted by a [100] RD Inverse Pole Figure (IPF) map. (b,d) are [001] ND IPF maps [9].

Figure 12. Microstructure of samples heated at 1500°C/s to 749°C (a,b), and to 862°C (c,d). The microstructure consists of a mixture of ferrite and martensite. Arrows indicate grains oriented close to the Goss {110}<001> (c,d), and circles the rotated Goss {110}<011> (a,b) components. (a,c) correspond to IQ maps in which the recrystallized grains of ferrite are highlighted by a [100] RD Inverse Pole Figure (IPF) map. (b,d) are [001] ND IPF maps [9].

3.3. Q&P steel samples: microstructures

Figure 13 a-d shows EBSD image quality maps (top) and phase maps (bottom) of samples heat treated according to the schedules of figure 3. The heating rate is mentioned under each map. The martensite grains in the conventionally Q&P heat treated samples are rather large (average grain diameter of 2.5 µm) with 14.1 % fresh martensite blocks, cf. Figure 13a. If a flash annealing process is conducted instead of an isothermal holding at 850°C, the microstructure is refined and the average grain diameter of the martensite reduces to 2 µm, (cf. Figure 13b). In this flash heat treatment, the austenite formation started in a fully recrystallized bcc matrix, but it can be seen that there was no time for all of the austenite grains to grow, resulting in a bimodal grain size distribution. Similar conclusions can be drawn after analyzing the microstructures obtained with a heating rate of 500°C/s, cf. Figure 13c. When the heating rate was increased from 500°C/s to 1000°C/s, the fresh martensite fraction decreased significantly due to the presence of 25% ferrite, cf. Figure 13d. The average bcc grain diameter reduced to 1.4 µm and the retained austenite grains became smaller and more homogenously distributed.

From the EBSD data, the approximate prior austenite grain size (PAGS) can be determined by plotting the rotation angles between 21.1° and 47.1° [19]. The linear interception method was used to determine the average PAGS for the Q&P samples as illustrated in Figure 13 (a-d bottom row). The average prior austenite grain diameter in the material after heating at 10°C/s and isothermal soaking is 3.8 µm and decreases to 2.9 µm without isothermal soaking. With a higher heating rate, the PAGS

diameter decreased to 1.7 μm for 1000°C/s. After the Q&P heat treatment cycle without soaking, the austenite and ferrite grain sizes decreased from 0.6 μm to 0.3 μm and from 2.0 μm to 1.4 μm, respectively, as the heating rate was increased from 10°C/s to 1000°C/s. Figure 14 shows the results of quantification of the PAGS, average BCC grain diameter and the grain size of retained austenite.
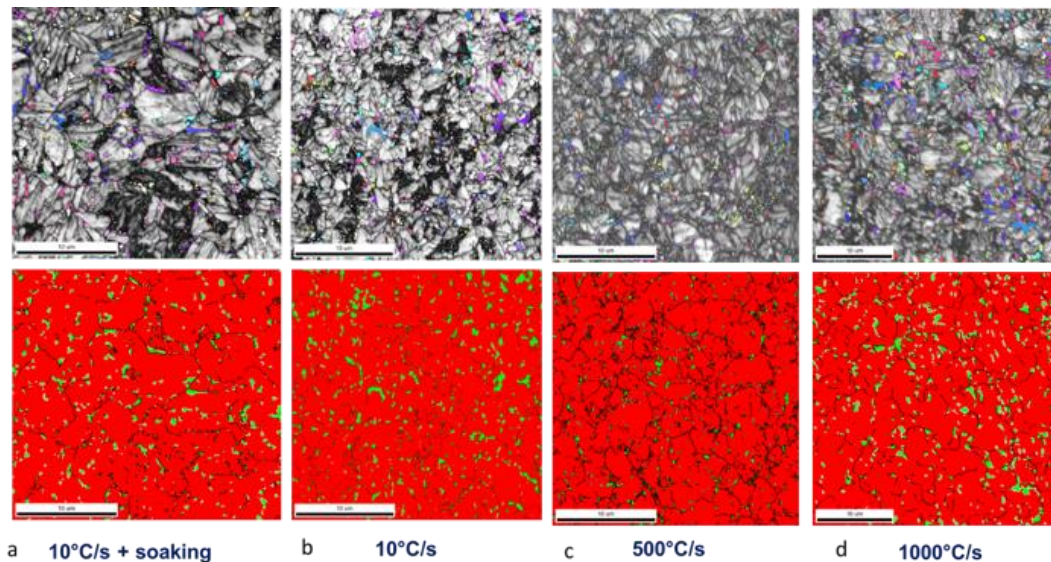
Figure 13. Image quality (IQ) maps top and phase maps (bottom) for samples Q&P with different heating rates and with and without isothermal soaking (Scale bars equal 10 *μm*). The black lines delineate the prior austenite grain boundaries derived according the work of Bernier et al. [19].

3.4. Q&P steel samples: textures
The textures of the samples were calculated from the EBSD data. Figure 14b displays the changes in the crystallographic textures as a function of the reheating rates. The texture of the cold rolled sample is characterized by an RD-ND fibre texture with a maximum of 8 mrd (multiples of a random distribution) on the {111}<112> texture component and a weaker rotated cube {100}<110> with an intensity of 4 mrd. The texture shows a convex curvature of the ND fibers, which is typical for cold rolled low carbon steels.

After reheating the cold rolled sample with 10°C/s and isothermal soaking, the cold rolling texture changes to a recrystallization type texture, which is characterized by a strong ND-fiber texture with a concave curvature and the disappearance of the RD-fiber component [20], cf. Figure 14b. Flash processing (i.e. without soaking) at 10°C/s changes the curvature of the ND-fiber from concave to straight as shown in Figure 14b. After increasing the heating rate to 500°C/s and 1000°C/s (cf. Figure 14b), the texture starts to resemble the original cold rolled texture with a convex curvature of the ND-fibers but with much lower intensity of ~4 mrd. Due to a texture memory effect, the martensite phase inherits the texture of the untransformed ferrite: we can conclude that this ferrite was not recrystallized but possibly only recovered [17]. Similar effects were reported by Senuma *et al*. [21] and Petrov *et al*. [6] in rapidly annealed cold-rolled extra low carbon and advanced high strength steel sheets, respectively.

3.5. Q&P steel samples: mechanical properties
Representative examples of the stress strain curves of the conventionally heat treated Q&P sample, and of samples heated at 10°C/s, 500°C/s and 1000°C/s without soaking are given in Figure 15a. The corresponding characteristic values are given in [8].

The conventionally Q&P heat treated sample has a uniform elongation of 6.1% with a yield strength and ultimate tensile strength of 782 MPa and 1050 MPa respectively. If the isothermal

soaking is removed after heating at 10°C/s, the uniform elongation decreases to 2.6% with higher yield and ultimate tensile strengths of 837 MPa and 1097 MPa, respectively. Increasing the heating rate to 500°C/s results in a uniform elongation of 8.6% with an ultimate tensile strength of 1,138 MPa and a heating rate of 1,000°C/s results in a uniform elongation of 12.8% with an increased yield and ultimate tensile strengths of 811 MPa and 1,318 MPa, respectively. The ratio of yield strength to ultimate tensile strength decreases with higher heating rates without soaking, cf. Table 1. The n-values were also calculated as 0.241 for a heating rate of 10°C/s, 0.167 for 500°C/s and 0.245 for 1000°C/s.

The fracture surface of the conventionally Q&P treated and the sample heated at 10°C/s without soaking is quasi-cleavage. Figure 15b (a-b) reveals some dimples but fracture propagated mostly by cleavage resulting in a mixed ductile-brittle fracture mode. After ultra-fast heating, fracture resulted in a ductile fracture surface with large dimples, cf. Figure 15b (c-d).
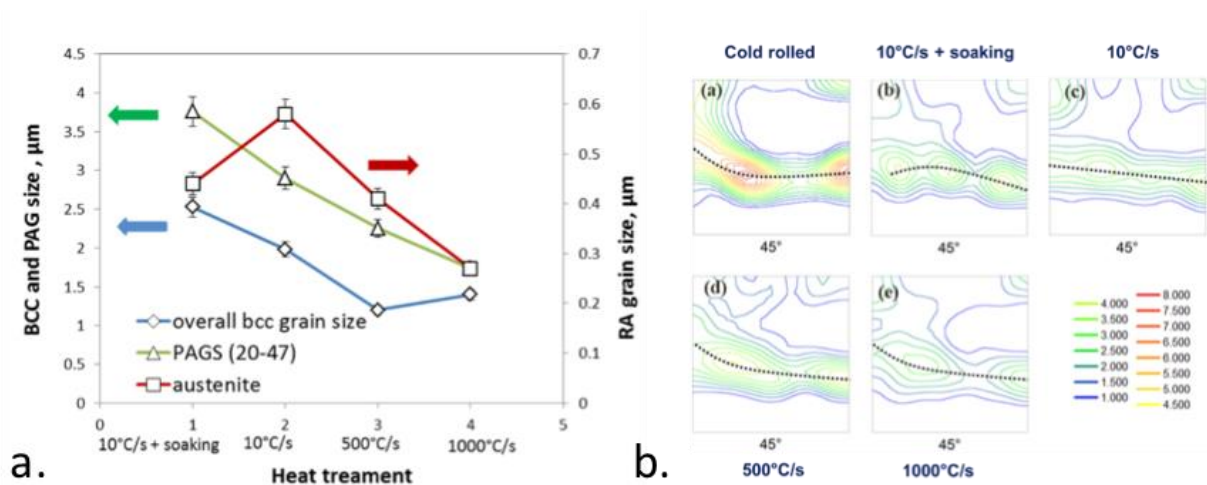
Figure 14 (a) Dependence of the average grain size from the heating rate and the isothermal soaking; (b) ODFs showing the texture evolution as a function of the heating rate and soaking time. The dotted line displays typical curvature of the ND fibres observed in cold rolled and recrystallized steels.
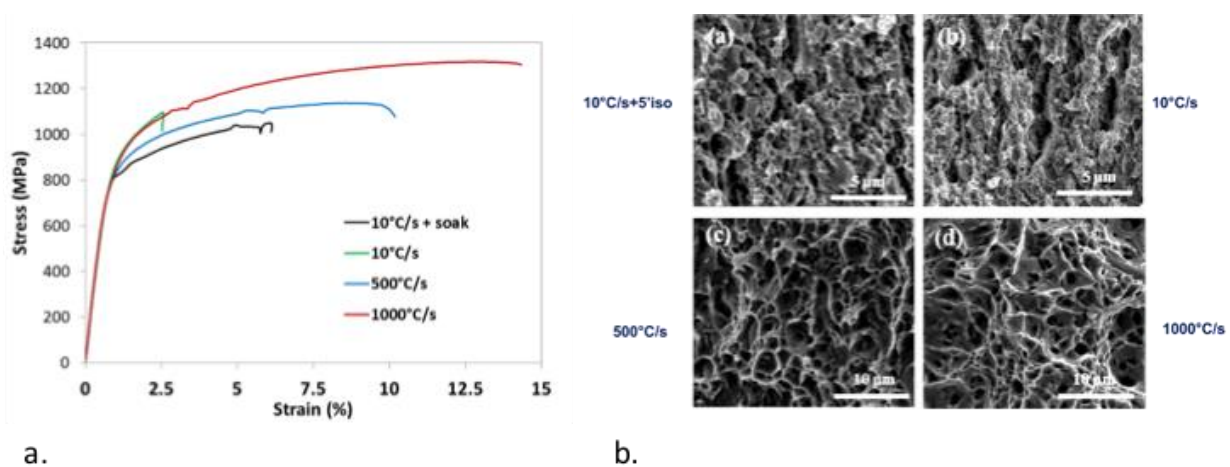
Figure 15. (a) Tensile test curves of samples after Q&P with different heating rates with and without isothermal soaking. (b) fracture surface of the samples (adapted from [8]).

4. Conclusions

The results in this study show that the microstructure and mechanical properties of existing AHSS compositions can be improved without addition of expensive alloying elements if fast heating without isothermal soaking is used. The most important findings in this study can be summarized as follows:

1. In both the DP and Q&P steels presently under investigation, the recrystallization after ultra-fast heating was not 100% complete before the onset of the α-to-γ transformation. The ultra-fast heating and the absence of the isothermal soaking produce a strong grain refinement effect in which the detailed features critically depend on the initial microstructure.

2. Ultra-fast annealing may induce an important texture shift as (i) it affects the volume fraction of ferrite that is recrystallized at the onset of α-to-γ transformation and (ii) it generally enhances oriented nucleation effects such as preferred low or high-stored energy nucleation because of an effect on the balance of driving force for recovery and nucleation.

3. The mechanical properties of the ultra-fast annealed DP and Q&P samples, with heating rates of 400°C/s, 500°C/s and 1000°C/s without isothermal soaking, are better than for the conventionally processed Q&P samples, combining an increase in strength up to 26% and ductility up to 134% (for Q&P) as compared to the conventional equivalents.

4. The fracture surface changes from quasi-cleavage in conventionally heat treated samples to ductile dimples in the ultra-fast annealed ones.

The results of the current study undoubtedly show that ultra-fast reheating of HSLA steels is a potential way to achieve significant strengthening with a minimum loss of ductility, and under certain conditions to achieve even an increase in ductility. The observed increases in strength were associated with a strong grain refinement caused by the overlapping of the α-to-γ phase transformation and ferrite recrystallization. These effects are observed also with heating rates of ~400°C/s, which can be obtained in an industrial processing line. The results also show that the control of the initial microstructures before cold rolling together with the heating rates is of crucial importance for designing HSLA steels with improved mechanical properties, i.e. to effectively fill the gap in the strength vs. ductility chart, in the domain of strengths above 1,200 MPa and elongations of ~20%, without the use of expensive alloying additions.

References
[1] De Moor E, Gibbs P J, Speer J G, Matlock D K and Schroth J G 2010 Strategies for third-generation advanced high-strength steel development Iron and Steel Technology vol 7 pp 133–44
[2] De Cooman B C 2004 Structure-properties relationship in TRIP steels containing carbide-free bainite Curr. Opin. Solid State Mater. Sci. 8 285–303
[3] Senuma T 2001 Influence of the heating rate in an annealing process on the recrystallization behavior and texture formation of a cold rolled extralow carbon steel sheet Recrystallization and grain growth, vols. 1 and 2 ed D Gottstein, G and Molodov (Heidelberger platz 3, D-14197 Berlin, Germany: Springer-Verlag Berlin) pp 1125–30
[4] Reis A C da C, Bracke L, Petrov R, Kaluba W J and Kestens L 2003 Grain Refinement and Texture Change in Interstitial Free Steels after Severe Rolling and Ultra-short Annealing ISIJ Int. 43 1260–7
[5] Petrov R, Kestens L, Kaluba W and Houbaert Y 2003 Steel grips : journal of steel and related materials. vol 1(GRIPS media)
[6] Petrov R H, Sidor J and Kestens L A I 2012 Texture formation in high strength low alloy steel reheated with ultrafast heating rates Mater. Sci. Forum 702–703 798–801
[7] Petrov R, Kestens L and Houbaert Y 2001 Recrystallization of a Cold Rolled Trip-assisted Steel

during Reheating for Intercritical Annealling. Isij 41 883–90

[8]   De Knijf D, Puype A, Föjer C and Petrov R 2015 The influence of ultra-fast annealing prior to quenching and partitioning on the microstructure and mechanical properties Mater. Sci. Eng. A 627 182–90

[9]   Castro Cerda F, Kestens L, Monsalve A and Petrov R 2016 The Effect of Ultrafast Heating in Cold-Rolled Low Carbon Steel: Recrystallization and Texture Evolution Metals (Basel). 6 288

[10]   Kang J Y, Bacroix B, Réglé H, Oh K H and Lee H C 2007 Effect of deformation mode and grain orientation on misorientation development in a body-centered cubic steel Acta Mater. 55 4935–46

[11]   Ray R K, Jonas J J and Hook R E 1994 Cold rolling and annealing textures in low carbon and extra low carbon steels Int. Mater. Rev. 39 129–72

[12]   Hutchinson W B 1984 Development and control of annealing textures in low-carbon steels Int. Met. Rev. 29 25–42

[13]   Nguyen Minh T, Sidor J, Petrov R and Kestens L 2012 Occurrence of shear bands in rotated Goss ({110}<110>) orientations of metals with bcc crystal structure Scr. Mater. 67 935–8

[14]   Gobernado P, Petrov R H and Kestens L A I 2012 Recrystallized {311} ⟨136⟩ orientation in ferrite steels Scr. Mater. 66 623–6

[15]   Kang J-Y, Kim D-I and Lee H-C 2009 Texture Development in Low Carbon Sheet Steels for Automotive Application Microstructure and Texture in Steels (London: Springer London) pp 85–101

[16]   Dillamore I L, Morris P L, Smith C J E and Hutchinson W B 1972 Transition Bands and Recrystallization in Metals Proc. R. Soc. London. Ser. A, Math. Phys. Sci. 329 405–20

[17]   Ushioda K, Hutchinson W B, Ågren J and von Schlippenbach U 1986 Investigation of structure and texture development during annealing of low-carbon steel Mater. Sci. Technol. 2 807–15

[18]   Castro Cerda F M, Vercruysse F, Minh T N, Kestens L, Monsalve A and Petrov R 2017 The Effect of Heating Rate on the Recrystallization Behavior in Cold Rolled Ultra Low Carbon Steel Steel Res. Int. 88

[19]   Bernier N, Bracke L, Malet L and Godet S 2014 An alternative to the crystallographic reconstruction of austenite in steels Mater. Charact. 89 23–32

[20]   Farideh HajyAkbary 2015 Optimising mechanical behaviour of new advanced steels based on fine non-equilibrium microstructures (TU Delft)

[21]   Senuma T, Kawasaki K and Takemoto Y 2006 Recrystallization Behavior and Texture Formation of Rapidly Annealed Cold-Rolled Extralow Carbon Steel Sheets Mater. Trans. 47 1769–75

[22]   Petrov R.H., Kestens L.A.I., Colás R., Totten G.E. (Eds.), Advanced High-strength Steels: Electron Backscatter Diffraction (EBSD), CRC Press, 2016, pp. 46–69 Encycl. Iron, Steel, and Their Alloys. http://dx.doi.org/10.1081/E- EISA-120050786

[23]   Castro Cerda F.M., Goulas C., Sabirov I., Kestens L.A.I. and Petrov R.H. 2017, The effect of the pre-heating stage on the microstructure and texture of a cold rolled FeCMnAlSi steel under conventional and ultrafast heating, Mater. Charact. doi:10.1016/j.matchar.2017. 06.010, in press